

A scalable, efficient, and facile ambient drying approach for preparing low shrinkage, compressive, and super porous nano cellulose-based aerogel via a physicochemical crosslinking strategy

Chunxia Tang^{a*}, Jing Yang^a, Jian Liu^a, Yunshan Mao^a, Shaohai Fu^a

a College of Textile Science & Engineering, Jiangnan University, 1800 Lihu Avenue, Wuxi, Jiangsu 214122, China

Corresponding author:

Dr. Chunxia Tang

E-mail: chunxia.tang@jiangnan.edu.cn

Postal address: College of Textile Science & Engineering, Jiangnan University, 1800 Lihu Avenue, Wuxi, Jiangsu 214122, China

Other authors:

Jing Yang, E-mail: 6223014002@stu.jiangnan.edu.cn

Postal address: College of Textile Science & Engineering, Jiangnan University, 1800 Lihu Avenue, Wuxi, Jiangsu 214122, China

Jian Liu, E-mail: 15047641128@163.com

Postal address: College of Textile Science & Engineering, Jiangnan University, 1800 Lihu Avenue, Wuxi, Jiangsu 214122, China

Yunshan Mao, E-mail: mys991213@163.com

Postal address: College of Textile Science & Engineering, Jiangnan University, 1800 Lihu Avenue, Wuxi, Jiangsu 214122, China

Shaohai Fu, E-mail: shaohaifu@hotmail.com

Postal address: College of Textile Science & Engineering, Jiangnan University, 1800 Lihu Avenue, Wuxi, Jiangsu 214122, China

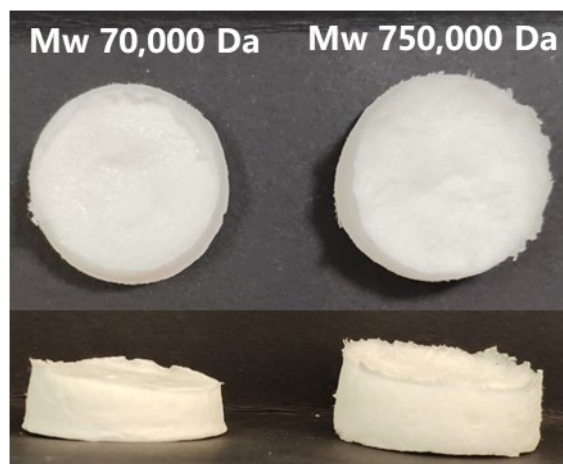


Figure S1. The digital photos of BGP1.0-2C aerogels prepared by PEI with Mws of 70,000 Da and 750,000 Da.

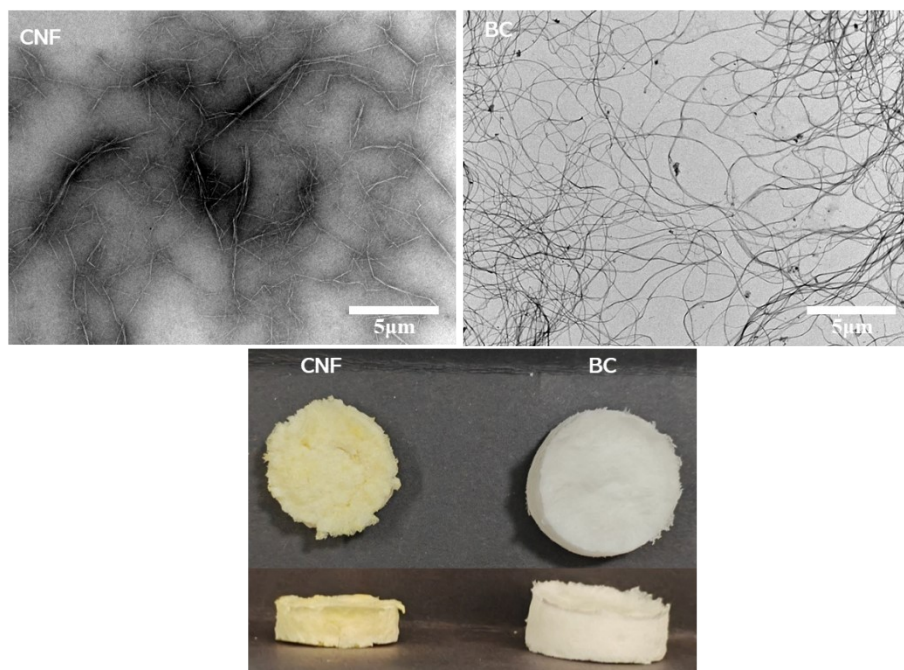


Figure S2. The TEM images of cellulose nanofibers with an average $<10\ \mu\text{m}$ (TEMPO-Oxidized cellulose nanofibrils) and $>20\ \mu\text{m}$ (Bacterial nanocellulose). The digital photos of aerogels prepared by cellulose nanofibers with different lengths.

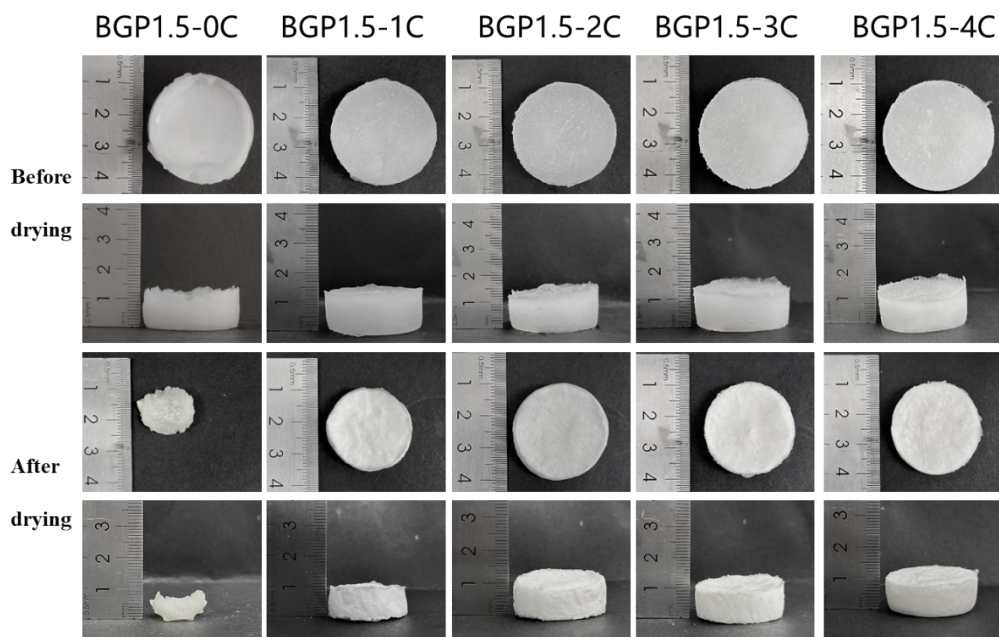


Figure S3. The digital photos of BGP1.5-xC gels before and after ambient drying.

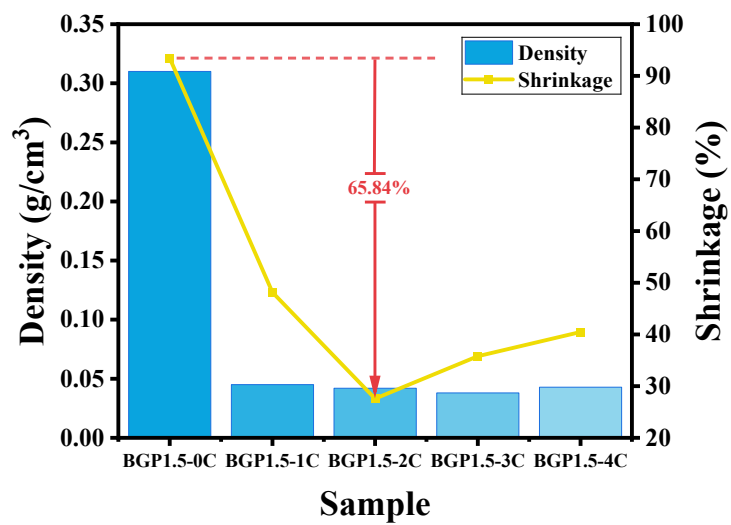


Figure S4. The bulk density and volume SR of BGP1.5-xC aerogels.

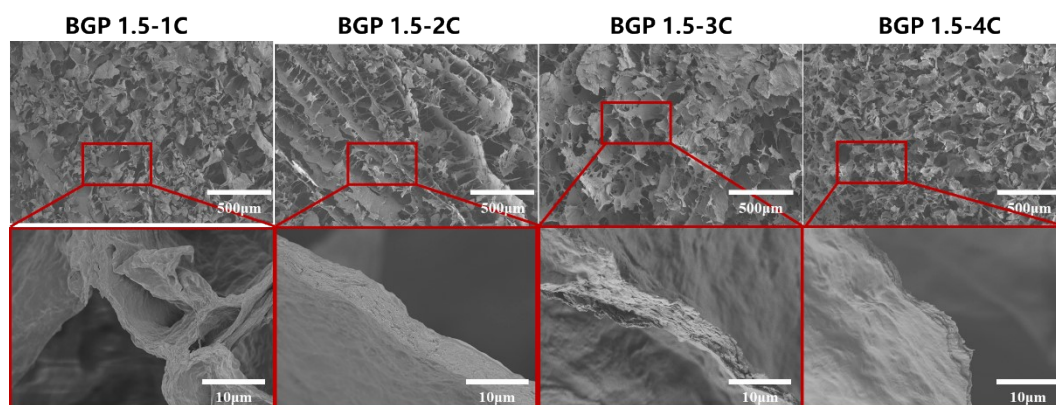


Figure S5. SEM images of BGP1.5-xC aerogels at different magnifications.

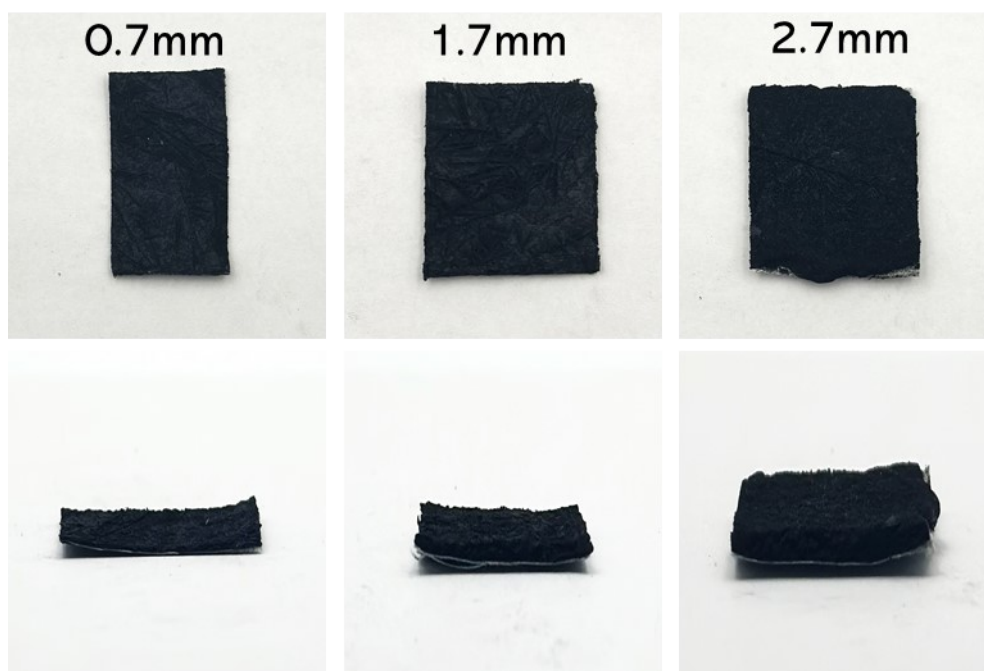


Figure S6. Digital photos of BGP-MXene aerogel with different thickness functionalized fabrics.

Table S1. Langmuir and Freundlich adsorption constants of BGP for Cr(VI) adsorption

Isotherm models	Parameters	
Langmuir	q_m (mg/g)	426.31
	K_L (L/mg)	0.60
	R^2	0.95
Freundlich	K_F (mg/g/mg/L) ^{1/n}	175.10
	n	4.81
	R^2	0.88

Table S2. The parameters of pseudo-first-order and pseudo-second-order kinetic models for Cr(VI) adsorption onto BGP.

	PFO			PSO		
	Qe (mg/g)	K_1	R^2	Qe (mg/g)	K_2	R^2
BGP	328.71	0.065	0.94	342.17	2.86×10^{-4}	0.99

Table S3. The parameters of intra-particle diffusion model for Cr(VI) adsorption onto BGP.

	Intra-particle diffusion model					
	$K_{id,1}$	$K_{id,2}$	$K_{id,3}$	C_1	C_2	C_3
BGP	54.89	16.12	1.22	2.32	138.98	302.89